Present and Future of Modeling Global Environmental Change: Toward Integrated Modeling,
Eds., T. Matsuno and H. Kida, pp. 111–136.

Macroscale Hydrology: Challenges and Opportunities

Dennis P. LETTENMAIER

Department of Civil and Environmental Engineering, University of Washington, Seattle, WA 98195, U.S.A.

Abstract—Understanding the hydrologic response of very large river basins offers new challenges and opportunities for hydrologists. Traditionally, hydrologists have tended to focus on catchments or watersheds ranging from plot scale research sites (typically o(10^{-2} km^2)), to small experimental catchments (0.1–10 km^2), and occasionally medium sized catchments (10^2–10^3 km^2). As the understanding of the role of the land surface as represented in coupled land-atmosphere-ocean models has evolved so has the need for hydrologic models applicable to large areas and river basins. This paper describes development of the Variable Infiltration Capacity (VIC) macroscale hydrology model, and its application to environmental issues associated with land use and climate change prediction, and medium range hydrologic forecasting.

The distinguishing hydrologic features of VIC as compared to other land surface models are its representation of the subgrid variability in soil moisture storage capacity as a spatial probability distribution, and its representation of base flow as a nonlinear recession. In contrast with more conventional hydrologic models, VIC explicitly represents vegetation, and simultaneously solves the surface energy and water balances. In common with most hydrologic models, a river routing model permits comparisons between the model-derived discharge and observations at gauging stations.

The VIC model has been applied to evaluate the hydrologic implications of global warming on large continental rivers. An assessment of nine large river basins (Amur, Mackenzie, Mekong, Mississippi, Severnaya Dvina, Xi, Yellow, Yenisei) which span a range of hydroclimatic conditions is described. The largest predicted changes in the hydrological cycle were for the snow-dominated river basins of mid to higher latitudes, and are attributable in part to the greater amount of warming predicted for these regions, but more importantly, to the central role of snow in the water balance. The model has also been used to assess the hydrological effects of vegetation change. An application to the Columbia River Basin of northwestern North America is described, using reconstructed vegetation for 1900, and a recent vegetation inventory. For this application, the model was implemented at 1/4 degree spatial resolution, using 1 km resolution vegetation data for current conditions, and a reconstructed 1900 vegetation scenario. The results show that, hydrologically, the most important vegetation-related change has been a general tendency toward decreased vegetation maturity in the forested areas of the basin, which represents a balance between the effects of logging and fire suppression. This results in slight predicted increases in runoff, and decreases in evapotranspiration, although on an annual average basis the changes are quite small, mostly less than 5%. Finally, the model has been applied to develop ensemble streamflow forecasts for large river basins. The example shown is an application to the eastern and central U.S. during summer, 2000. Ensemble climate forecasts (precipitation and average temperature for six-month lead times, updated monthly), produced by the NCEP/CPC Global Spectral Model (GSM) were downscaled using a method that removes climate model bias at the 1/8 degree horizontal resolution at which the VIC model was implemented. Various aspects of the application are discussed, particularly the use of a method of downscaling the climate forecast information that removes the effects of bias in the climate model.

INTRODUCTION

The traditional realm of hydrologic models has been the prediction of streamflow. In the early days of digital computing, Crawford and Linsley (1960) developed the Stanford Watershed Model, which represented the runoff response of the land surface to surface meteorological forcings (especially precipitation). The conceptual representations within the model effectively considered the entire catchment area in a spatially lumped fashion, with multiple subsurface storage zones representing the nonlinearities, based on antecedent soil moisture, in the partitioning of precipitation into a “fast” runoff response, and infiltration. The major breakthrough in this model was its time-continuous construct, which avoided the necessity to specify antecedent conditions (soil moisture) at the onset of a storm, as did most of the then-existing “event models”. Variations of the Stanford Watershed Model remain in use today; both the U.S. National Weather Service River Forecast System and HSPF (Hydrologic Simulation Package-Fortran) are derivatives of the Stanford Watershed Model. This generation of so-called “conceptual simulation models” relies on a calibration procedure to estimate a number (usually 10–20) of site-specific parameters, either via manual or automated procedures that minimize the difference between model predictions and observations over a specified calibration period. Efforts to relate the parameters of this type of models to physically measurable quantities have generally been unsuccessful. Also, while such models can be quite useful for simulation of streamflow within the range of conditions for which they are calibrated, their applicability to altered conditions—either of land cover or climate—is limited. Furthermore, most such models do not represent the effects of vegetation on evapotranspiration explicitly, nor do they close the surface energy balance.

The terrestrial ecology community, on the other hand, over the last 20 years has developed models known as soil-vegetation-atmosphere transfer schemes (SVATS). Many of these models have been explicitly designed to represent the land surface partitioning of net radiation into latent, sensible, and ground heat fluxes in climate (and later, numerical weather prediction) models. In addition to representing the role of vegetation in evapotranspiration, these models close the surface energy balance, usually by iterating on one or more effective temperatures. However, as pointed out by Wood (1991), SVATS give much more attention to representation of column processes (extraction by vegetation of soil moisture, and feedbacks between vegetation, soil moisture, and surface atmospheric conditions that control transpiration) than they do to horizontal complexity (in soils and topography) that control runoff generation. Over the last decade, hydrologic models, which parameterize the processes affecting runoff generation, and SVATS, which close the water and energy balances and describe in some detail vegetation controls on evapotranspiration, have begun to converge. We describe here a hydrologically based macroscale land surface model (designed for application at horizontal resolutions ranging from fractional to multiple degrees latitude by longitude) which combines elements of both hereditary lineages. Development of the Variable Infiltration Capacity (VIC) model, as well as its application, are described though three examples. These are 1) effects of climate change on the hydrology of major continental rivers; 2) effects of vegetation change on the hydrology of the Columbia Rivers system (U.S. and Canada), and 3) development and testing of a hydrologic ensemble river forecast system.

VIC LAND SURFACE MODEL

VIC macroscale energy and water balance model has been developed over the last 10 years at the University of Washington and Princeton University. The first version of the VIC model is described in detail by Liang *et al.* (1994) and Liang *et al.* (1996a). As compared to other land surface models, VIC's distinguishing hydrologic features are a) its representation of subgrid variability in soil moisture storage capacity as a spatial probability distribution, to which surface runoff is related (Zhao *et al.*, 1980), and b) its parameterization of base flow, which occurs from a lower soil moisture zone as a nonlinear recession (Dumenil and Todini, 1992). As discussed by Lohmann *et al.* (1998a, b) the representation of soil hydrology (soil water storage, surface runoff generation and sub-surface drainage) has a critical influence on the predicted long-term water and energy balances.

The parameterization of spatial variability in soil properties, and topographic effects is based on a simplifying assumption that the large-scale effects can be represented adequately without assigning infiltration parameters to specific subgrid locations. The parameterized infiltration curve can also be interpreted as representing the fraction of a grid cell that contributes runoff via a "fast" response mechanism, such as saturation excess or fast subsurface flow. Movement of moisture between the soil layers is modeled as gravity drainage, with the unsaturated hydraulic conductivity a function of the degree of saturation of the soil (Campbell, 1974). The deepest soil layer produces base flow according to the base flow formulation of Todini (1996). In this way, the model separates subsurface flow from quick storm response.

Horizontally, the land surface is described by a number of land cover classes. The subsurface is characterized vertically by two or three soil layers. The land cover (vegetation) classes are specified by the fraction of the grid cell which they occupy, with their leaf area index (LAI), canopy resistance, and relative fraction of roots in each of the soil layers. Evapotranspiration from each vegetation type is calculated using a Penman-Monteith formulation with adjustments to canopy conductance to account for environmental factors following Jarvis (1976). The moisture fluxes between the soil layers, and the amount of evapotranspiration and runoff vary with the vegetation cover class. Evapotranspiration, surface runoff and base flow are computed for each cover type and summed over all cover types within a grid cell weighted by the fractional area that each cover type occupies.

The earliest version of the model was developed using point observational data from the ABRACOS site in Brazil and the First ISLSCP Field Experiment (FIFE) (Liang *et al.*, 1994). VIC has been evaluated in various phases of the WCRP PILPS (Project for Intercomparison of Land Parameterization Schemes) project (see Pitman *et al.*, 1993; Chen *et al.*, 1997; Liang *et al.*, 1996b; Wood *et al.*, 1998). Based on the PILPS results and applications to large-scale river basins reported by Abdulla *et al.* (1996), Wood *et al.* (1997), and Nijssen *et al.* (1997) the model parameterizations have been modified to include:

Thin surface layer

Results in PILPS-2b simulations of HAPEX-MOBILY demonstrated that a thin surface soil layer improved the model results during the summer period when dry conditions result in a soil control on evapotranspiration. The formulation and improvements are reported in Liang *et al.* (1996b). This PILPS/HAPEX analysis resulted in the three layer version of the model (VIC) that has been used in our most recent work, and will be used for the proposed project.

Improved ground heat flux parameterization

Accurate ground heat flux and surface temperature calculations are critical for accurate estimates of the other fluxes in the water and energy balance. Peters-Lidard *et al.* (1998) showed that the widely used McCumber and Pielke (1981) estimates of soil heat conductance can be better represented by using a formulation suggested by Johansen (1975). This parameterization, described by Liang *et al.* (1999) is now used in the model.

Sub-grid precipitation

Shuttleworth (1996) and others have shown the importance of including sub-grid precipitation representation within land surface models. An efficient parameterization has been developed, and incorporated in the model by Liang *et al.* (1996a).

Improved snow representation

The two-layer snow accumulation and ablation model of Wigmosta *et al.* (1994) as modified by Storck and Lettenmaier (1999) has been incorporated in VIC, replacing the earlier temperature index method. The effect of vegetation cover on snow accumulation and melt is represented via an energy balance approach, applied both to snow intercepted by the canopy, and to the underlying snowpack. The effect of shortwave attenuation of solar radiation by the vegetation canopy, and re-radiation as longwave, is also represented. Subgrid variations in snow accumulation and ablation are accounted for through use of snow elevation bands.

Soil freeze-thaw processes

Betts *et al*. (1998) showed, based on BOREAS data, how biases in forecasts of temperature over land can result from failure to characterize properly the effects of soil thermal processes. Soil freezing, in particular, tends to radically alter the Bowen ratio, especially during thaw periods, and can strongly affect runoff generation. Cherkauer and Lettenmaier (1999) describe an algorithm, now incorporated in the VIC model, which represents the effect of soil freeze-thaw processes on heat flux and moisture movement through frozen soils.

River routing

River basins are modeled as grids (each with sub-grid variability in soil infiltration capacity, vegetation, precipitation, etc.) which have varied from 1/8 to 2 degrees, depending on the application. To compare model-derived to observed discharge, a routing model represents the time distribution for runoff reaching the outlet of each grid cell as well as the transport of water through the open channel (river) system. The inclusion of the river routing model, developed by Lohmann *et al*. (1998a, b) permits comparisons between the model-derived discharge and observations at gauging stations.

Model evaluation

Over the last 5 years, the VIC model has been tested and applied at a range of spatial scales, from large river basins to continental and global scales. These studies have been reported in Abdulla *et al*. (1996), Nijssen *et al*. (1997), Wood *et al*. (1997), Wood *et al*. (1998), O'Donnell *et al*. (2000), and Nijssen *et al*. (2001a, b). VIC participated in the PILPS project, including the PILPS-2c intercomparison for the 566,000 km^2 Red-Arkansas River basins, which used 10-year, 3-hourly model forcing data (see Wood *et al*., 1998). The model is currently participating in the PILPS-2e Arctic Hydrology Model Intercomparison Project (http://www.hydro.washington.edu/Lettenmaier/CurrentResearch/PILPS-2e/index.htm).

Detailed diagnosis of VIC model results has been carried out over the central U.S. by Maurer *et al*. (2001a) as part of the Land Data Assimilation System (LDAS) project, which includes retrospective simulations (eventually for 50 years) for long-term validation against basin discharge and to test model parameterizations. Figure 1 shows selected results for the major tributary basins within the Mississippi basin. The simulations were carried out on the LDAS 1/8 degree at a 3 hourly time step.

Comparisons have also been made between the volumetric soil moisture and the State of Illinois soil moisture network. Figure 2, from Maurer *et al*. (2001b) shows good agreement between the spatially averaged station soil moisture and simulations from the VIC model, especially for the change in soil moisture (middle panel) and the monthly autocorrelation (bottom panel). The top panel, which presents the absolute volumetric soil moisture, shows a difference between the observations (top line and bars to show the range among the stations) and the average soil moisture for the modeled grid boxes. This difference is due in part from the well-known result that models tend to have their own "climatology"

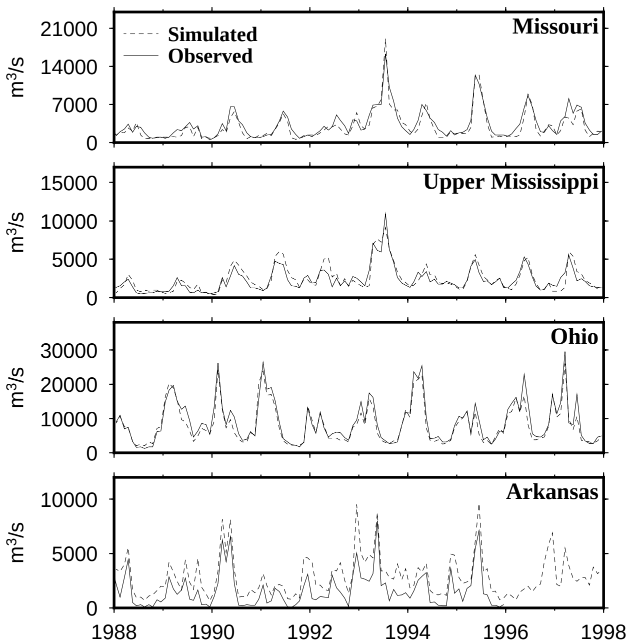

Fig. 1. Simulated and observed discharge for major Mississippi River tributaries (from Maurer *et al*., 2001a).

(Koster and Milly, 1997) and in part to the differences between the measurement scale (points) and modeling scale (1/8th degree). Such systematic effects can be removed (see Wood *et al*., 2001) by establishing VIC's model climatology. What is encouraging is the excellent model agreement with the observed moisture flux (change in soil moisture) over an annual cycle. The validation studies give us confidence that the VIC land surface model can provide fields of surface hydrologic states (soil moisture, surface temperature and snow extent and water equivalent) of sufficient accuracy to allow simulations of synthetic satellite observations.

CASE STUDY 1: GLOBAL RIVER SENSITIVITY TO CLIMATE CHANGE

Changes in land surface hydrology due to changing climate have potentially far reaching implications both for human populations and for regional-scale physical and ecological processes. The geographic and topographic characteristics of large river basins and the climatic variations that determine their hydrologic characteristics often constitute the defining features of the regions they occupy. They govern to a considerable extent the development of ecosystems, as well as human communities and their activities. These regional ecosystems and human activities are usually reasonably well adapted to the current climate conditions, but may be vulnerable to large or rapid changes in climate.

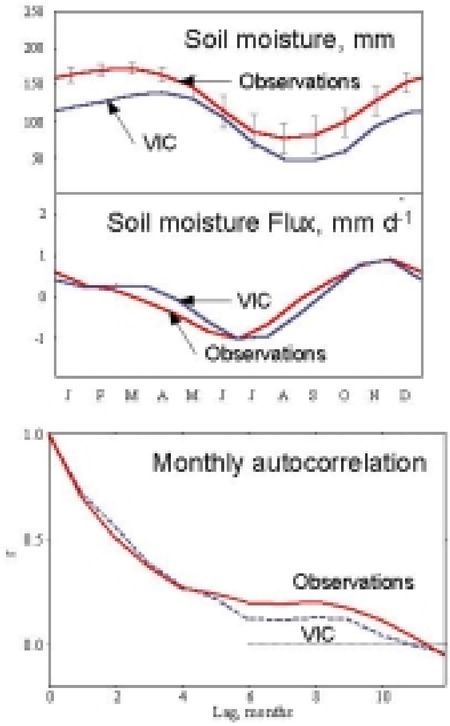

Fig. 2. Comparisons between VIC soil moisture simulations and observations from the Illinois soil moisture network (from Maurer *et al*., 2001b).

Many studies of the impact of climate change on water resources for specific geographic regions have been reported. Gleick (1999), for example, compiled a bibliography of more than 800 papers addressing the impacts of climate change on U.S. water resources. Arnell (1999) studied the effect of climate change on hydrological regimes in Europe, and numerous other studies have been conducted elsewhere. However, there has been less effort to place the regional hydrological consequences of climate predictions in a global context. In attempting to do so, Nijssen *et al*. (2001c) targeted nine large river basins, selected to represent a range of geographic and climatic conditions. Figure 3 shows the location of the nine river basins. Changes in precipitation and temperature were calculated based on altered climate simulations produced by long (multi-decadal) runs of four global General Circulation Models (GCMs), which have been widely used in climate impact scenario analysis (see, e.g., Felzer and Heard, 1999).

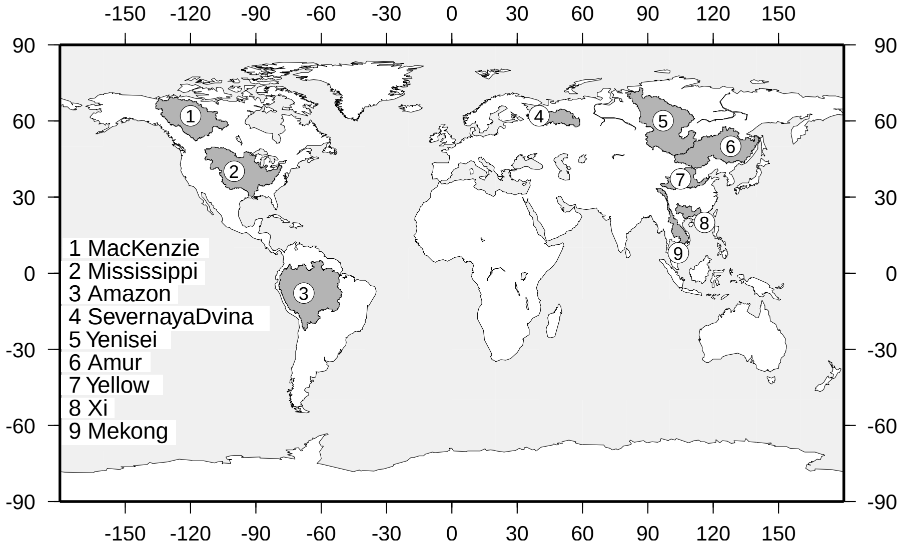

Fig. 3. Location of the nine selected river basins (from Nijssen *et al*., 2001c).

Climate scenarios from eight GCMs were obtained from the Intergovernmental Panel on Climate Change Data Distribution Center (IPCC-DDC). All eight models are coupled ocean-atmosphere models, output from which was archived as part of the IPCC climate change efforts. Figure 4 shows the predicted changes in mean annual temperature and precipitation for each of four GCMs for which output was obtained for the nine basins for the decades centered on 2025, 2045, and 2095. All models predict progressive warming for all basins. Not unexpectedly, the spread between the models increases with an increase in the lead time of the prediction. Some of the differences are likely attributable to the differences in the emission scenarios, although relationships between the magnitude of warming and the emissions scenarios used is not clear. Predicted annual average warming ranges from 0.8°C for the Xi (HCCPR-CM2) in 2025 to 8.5°C for the Mackenzie (CCSR-CGCM) in 2095. All models predict an increase of precipitation for the northern basins (Mackenzie, Severnaya Dvina, and Yenisei), but the signal is mixed for basins in the mid-latitudes and tropics. Predicted changes in precipitation range from –30.3% for the Xi (CCCMA-CGCM) in 2095 to 27.6% for the Mackenzie (CSIRO-CGCM), also in 2095.

The hydrologic modeling used results from four of the climate models (HCCPR-CM2, HCCPR-CM3, MPI-ECHAM4, and DOE-PCM3) and two decades (2025 and 2045). These four models were selected because they offer the greatest spatial resolution, facilitating the downscaling step to the $2° \times 2°$ resolution of the hydrology models. More importantly, these four models include modern and relatively sophisticated land surface schemes that represent explicitly the interactions between vegetation and the surface energy and moisture budgets.

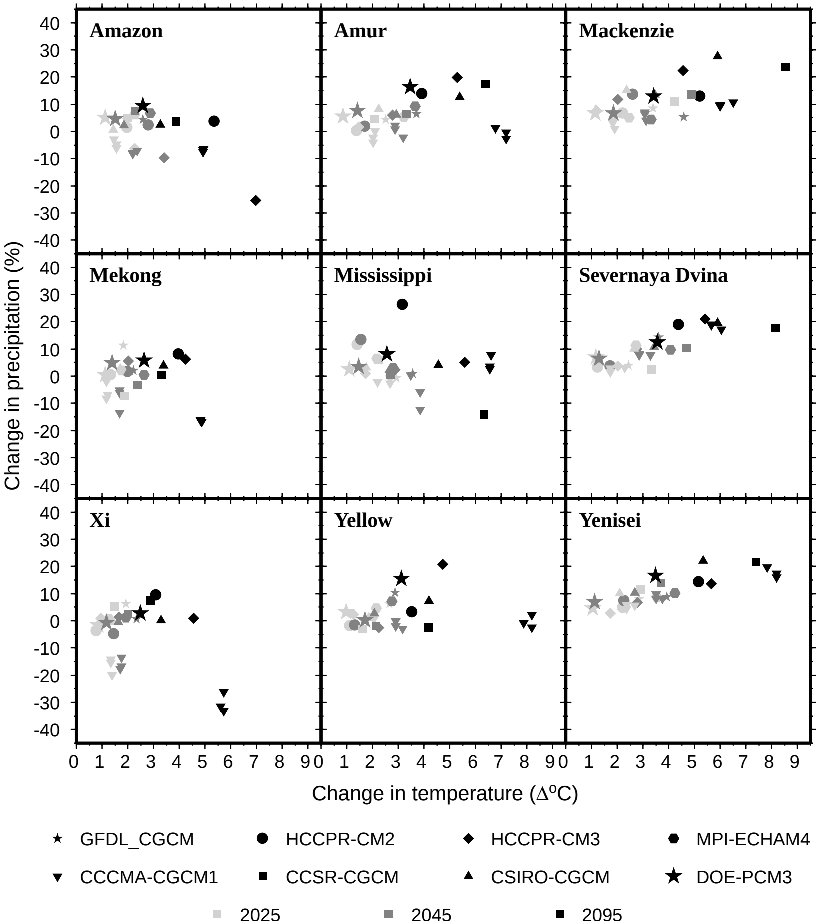

Fig. 4. Predicted changes in mean annual temperature and precipitation for each river basin for decades centered on 2025, 2045, and 2095. Climate predictions were not available for some models for 2095. For CCCMA-CGCM means from three ensembles for each decade are plotted (from Nijssen *et al.*, 2001c).

The decades 2025 and 2045 were selected for two reasons. First, in 2095 the spread in the predicted changes in temperature and precipitation is much larger than in the other two decades and some of the predicted changes in temperature are very large, even for these four models (e.g. 7.0°C warming for the Amazon in 2095 (HCCPR-CM3)). Second, planning horizons in water resources development are more typically on the order of 20–30 years, placing a greater emphasis on the decades 2025 and 2045.

A baseline simulation was performed, which acts as a surrogate for the real system under current climate conditions. In the baseline simulation the VIC model was forced with a global $2° \times 2°$ gridded data set of daily temperature and precipitation for the period 1979–1993. The remaining model forcings (vapor pressure, downward shortwave radiation, and net longwave radiation) were calculated by the VIC model using daily temperature, temperature range, and precipitation using algorithms by Kimball *et al*. (1997), Thornton and Running (1999), and Bras (1990). Daily surface wind speeds were obtained from the NCEP/NCAR reanalysis project (Kalnay *et al*., 1996). Subsequently, all changes in hydrological fluxes and storages were calculated relative to the baseline simulation. Results from previous work by Nijssen *et al*. (2001a, b) were used to estimate model parameters for the baseline simulations.

The daily data were used to drive the VIC model to calculate a set of derived variables (evapotranspiration, runoff, snow water equivalent, and soil moisture) and to study the water balance of each of the continents. For each $2° \times 2°$ model grid cell land surface characteristics such as elevation, soil, and vegetation were specified. Elevation data were calculated based on the 5 minute TerrainBase Digital Elevation Model (DEM) (Row *et al*., 1995), using the land surface mask from Graham *et al*. (1999). Vegetation types were extracted from the 1 km, global land classification of Hansen *et al*. (2000). Vegetation parameters such as height and minimum stomatal resistance were assigned to each individual vegetation class. Soil textural information and soil bulk densities were derived from the 5 minute FAO-UNESCO digital soil map of the world (FAO, 1995), combined with the WISE pedon data base (Batjes, 1995). The remaining soil characteristics, such as porosity, saturated hydraulic conductivity, and the exponent for the unsaturated hydraulic conductivity equation were based on Cosby *et al*. (1984).

From the archived GCM model output, mean monthly changes for decades 2025 and 2045 were computed relative to current climate simulations for each GCM. The monthly precipitation and temperature changes were used to alter the current climate hydrology model forcings, for the period of record of the observations (1979–1993). Results summarized in Nijssen *et al*. (2001c) show that the largest precipitation and temperature changes are generally for the northernmost basins. Furthermore, changes for the decade centered on 2045 are generally larger than for 2025, especially for temperature. Generally, the increases in temperature for the tropical and mid-latitude basins (Amazon, Mekong, Xi, and Mississippi) are fairly evenly distributed throughout the year. For the high-latitude basins, the temperature increases have a strong seasonal signal for most of the models, with the largest increases in temperature predicted for the winter months. However, there is considerable variation among GCMs in the change predicted by the GCMs, especially on a monthly basis. The predicted relative changes in precipitation likewise have their largest increases during the winter months for high-latitude basins. However, in some of these basins the precipitation falls mainly in the summer, and a small relative change in summer might amount to a larger change in annual precipitation volume than a large relative change in winter.

Figures 5 and 6 show the mean monthly simulated hydrographs for the nine basins, both for the baseline conditions and the four climate models for 2025 and

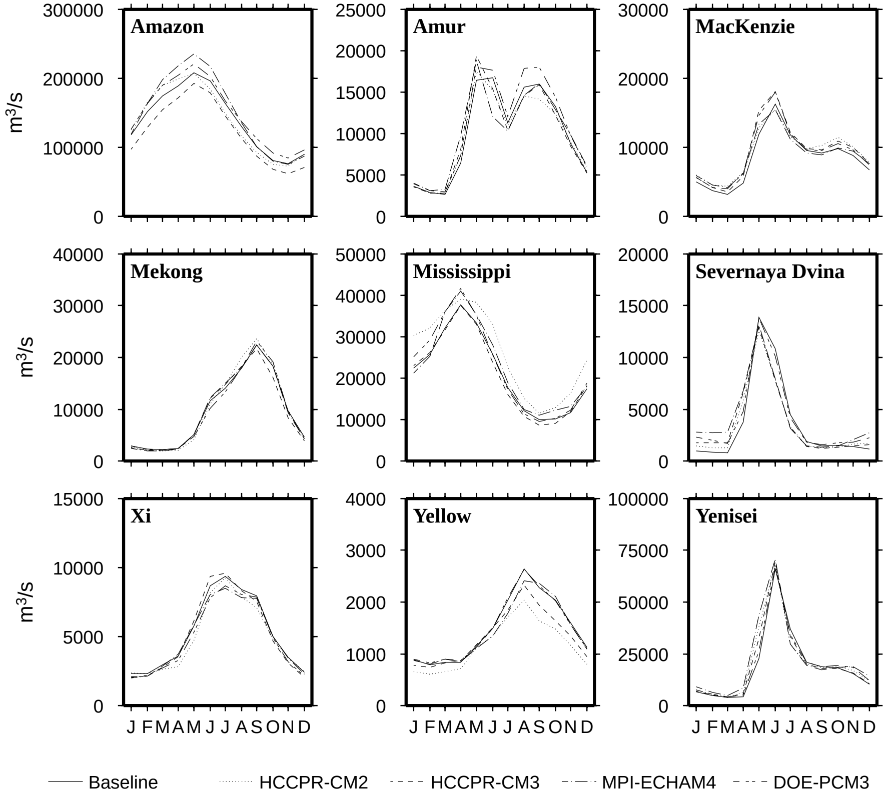

Fig. 5. Mean monthly hydrographs for baseline and climate model simulations for decade centered on 2025 (from Nijssen *et al.*, 2001).

2045, respectively. Although there is a large spread in predicted outcomes for most of the rivers, some general patterns are apparent. The Yellow River in Southeast Asia was the only river for which a reduction in annual streamflow resulted for all of the climate models in both decades—even for the MPI-ECHAM4 model in 2045, which predicted an increase in annual precipitation of 7.0% (from 517 to 553 mm). In this case, the increase in precipitation was offset by an increase in annual evapotranspiration of 9.3% (from 410 mm to 448 mm), caused by an increase in annual temperature of 2.7°C. Consequently, the VIC model predicted a small decrease in annual runoff of 1% (from 106 to 105 mm).

The tropical and mid-latitude basins generally do not show a change in the seasonal hydrographs, other than a general wetting or drying, depending on whether the change in temperature and the resulting increase in evapotranspiration are sufficient to offset the increase in precipitation. The exception is the HCCPR-CM2 simulation for the Xi river basin in 2045, which shows a large reduction in streamflow during the second half of the year, resulting from a 22% reduction in precipitation (from 649 to 508 mm) during the last six months of the year.

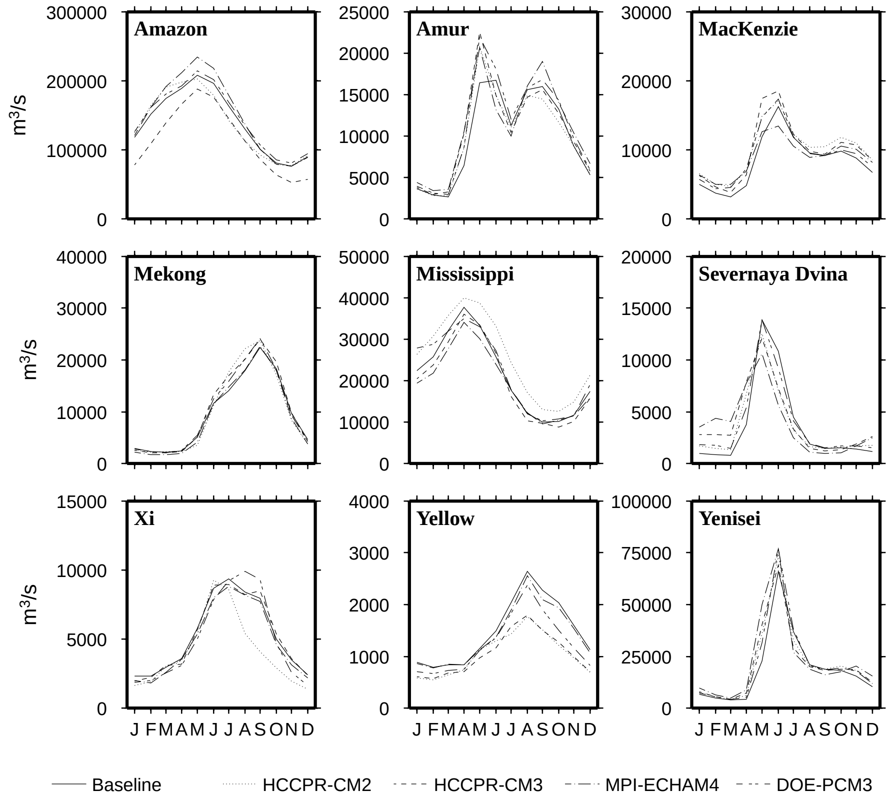

Fig. 6. Mean monthly hydrographs for baseline and climate model simulations for decade centered on 2045 (from Nijssen *et al.*, 2001).

One of the most persistent features of the predicted seasonal hydrographs occurs for those river basins in which a significant part of the annual precipitation falls in the form of snow under current climate conditions (Yenisei: 52%, Severnaya Dvina: 48%, Mackenzie: 41%, Amur: 21%). As mentioned above, the predicted warming in these high-latitude basins is greatest during the winter months. Consequently, a smaller amount of precipitation falls in the form of snow in the altered climate scenarios. This effect is most pronounced for those basins with large areas where the temperature is close to 0°C during part of the winter. For instance, the reduction in the amount of the precipitation falling in the form of snow is greater in the Severnaya Dvina than in either the Yenisei or the Mackenzie river basins, both of which experience very low temperatures during the winter.

In addition to a reduction in the amount of precipitation falling as snow, the model simulations generally show a delay in the start of snow accumulation and an advance in the onset of snow melt. Again, this is most pronounced for basins such as the Severnaya Dvina, where temperatures are not as cold as in the Yenisei or Mackenzie basins. For all basins where a significant part of the precipitation is stored as snow during the winter months, the hydrographs increase earlier in the spring under the altered climate scenarios. However, the warmer basins, such as the Severnaya Dvina, show a decrease in the spring peak flows despite an increase in winter precipitation as a result of shallower snow packs. The cold basins on the other hand show an increase in the spring peak flows, because almost all of the increase in winter precipitation is stored as snow during the winter months.

CASE STUDY 2: VEGETATION CHANGE EFFECTS ON HYDROLOGY

Human activity can dramatically alter land cover characteristics and subsequently hydrological and watershed processes. The effects of changes in land cover on the hydrology of small forested watersheds (drainage areas 1 to 1000 km^2) have been well documented (e.g., see Hibbert, 1967; Bosch and Hewlett, 1982; Harr, 1986; Jones and Grant, 1996; Stednick, 1996; Bowling and Lettenmaier, 1997). Removal of forest cover is known to increase streamflow as a result of reduced evapotranspiration and to increase peak flows due to higher water tables. In regions where snow processes are important, peak flows increase due to increased snow accumulation in clearings as compared to forested areas, and more rapid snow melt due to enhanced turbulent energy transfer in harvested areas (Storck, 2000).

The Columbia River drains an area of about 567,000 km^2, including portions of seven states in the western U.S., and part of British Columbia, in western Canada. Approximately 85% of the basin is within the U.S. and 15% is in Canada. The climate varies from moist, maritime conditions in the western parts of the basin to semiarid and arid conditions in the southeastern part. Topography exerts a strong control on precipitation within the basin. Mean annual precipitation varies from as much as 2500 mm/yr on the eastern slopes of the Washington Cascades, to as little as 200 mm/yr within the Columbia Plateau in Washington and the Snake River Plain in Idaho. In the mountainous headwater areas, most precipitation falls in the winter months as snow and is stored in deep snow packs during the winter. Spring snowmelt dominates the annual hydrograph of most tributaries, with approximately 60% of the runoff occurring in May, June, and July (Kirschbaum and Lettenmaier, 1997).

Mining and ranching were early mainstays of the local economies, supplemented by major timber production beginning in the early 1900’s (Quigley and Arbelide, 1997). For example, between 1899 and 1910, there was a 10-fold increase in timber production from Idaho. By 1986, timber harvest from within the U.S. portion of the basin represented about 27% of the total U.S. harvest. Summary statistics of land cover changes within the basin between 1900 and 1990 are presented in Section 5.1.

Substantial changes in land cover have occurred in the Columbia basin since extensive European settlement began in the mid-1800s. At lower elevations, which are primarily rangeland, there has been widespread conversion of native grasslands and shrublands to agriculture. Urbanization has decreased infiltration rates and increased the extent of impervious surfaces, although the area over which such changes has occurred is a small fraction of the total basin area. Most of the forested areas have been logged at least once. From a hydrologic standpoint, changes in forest cover most strongly affect the basin hydrology for two reasons. First, the spatial extent of forested areas is about three times greater than that of agricultural areas, and is much larger than that of urbanized areas. Second, forests occur in areas of higher precipitation and therefore contribute disproportionately to the water balance of the basin.

The federal Interior Columbia Basin Ecosystem Management Project (ICBEMP, Quigley *et al.*, 1997) developed vegetation scenarios for current (c. 1990) and 1900 conditions. For the Canadian portion of the basin, ICBEMP did not perform an historical vegetation reconstruction, and 1900 vegetation conditions were instead estimated using methods outlined in Kirschbaum and Lettenmaier (1997). Structural stage classes (related to vegetation maturity) created by Hardy *et al*. (1996) for the U.S. portion of the basin, and were extended to the Canadian portion as described by Kirschbaum and Lettenmaier (1997).

Figure 7 shows land cover classes for historical (1900) and current vegetation. The most apparent trends are conversion of grassland and shrubs to agriculture in the central part of the basin, and a general decrease in the maturity of forests over much of the basin. Areas historically dominated by grass and shrublands have been converted to agriculture and late-stage deciduous forests are essentially absent in the current vegetation map and middle-stage deciduous have increased slightly (to about 2% of the basin area). Further, while the spatial extent of coniferous forests has stayed constant (about 53% of the basin), there have been large shifts in structural stage. Late-stage coniferous forest have decreased about 21% from historical to current vegetation scenarios, with these decreases matched by increases in early-stage coniferous forests (up about 11%) and increases in middle-stage forests (up about 10%).

VIC model simulations were performed at 1/4 degree spatial resolution for a 10 year period, October 1979 to September 1989, using the same meteorological forcing data, soils, and topography and both the current and 1900 vegetation data. Topographic data were aggregated from 30 arc-second (approximately 1-km spatial resolution) USGS data. Daily precipitation and temperature minima and maxima were taken from a predecessor of the Land Data Assimilation System (LDAS) retrospective data (see Maurer *et al*., 2001a for details). Wind speed data were interpolated from the lowest vertical level of the NCEP-NCAR reanalysis (Kalnay *et al.*, 1996). Downward solar and longwave radiation and vapor pressure deficit were estimated from daily temperature range and temperature following methods described by Nijssen *et al*. (1997). The mean monthly flows using the current vegetation were in good agreement with the corresponding observed discharge, when adjusted for the effects of water management (Matheussen *et al*., 2000).

LAI is the most important vegetation characteristic that affects prediction of hydrologic responses. It is used in the VIC model in two ways. First, during periods of snow cover, the snow accumulation and ablation model characterizes

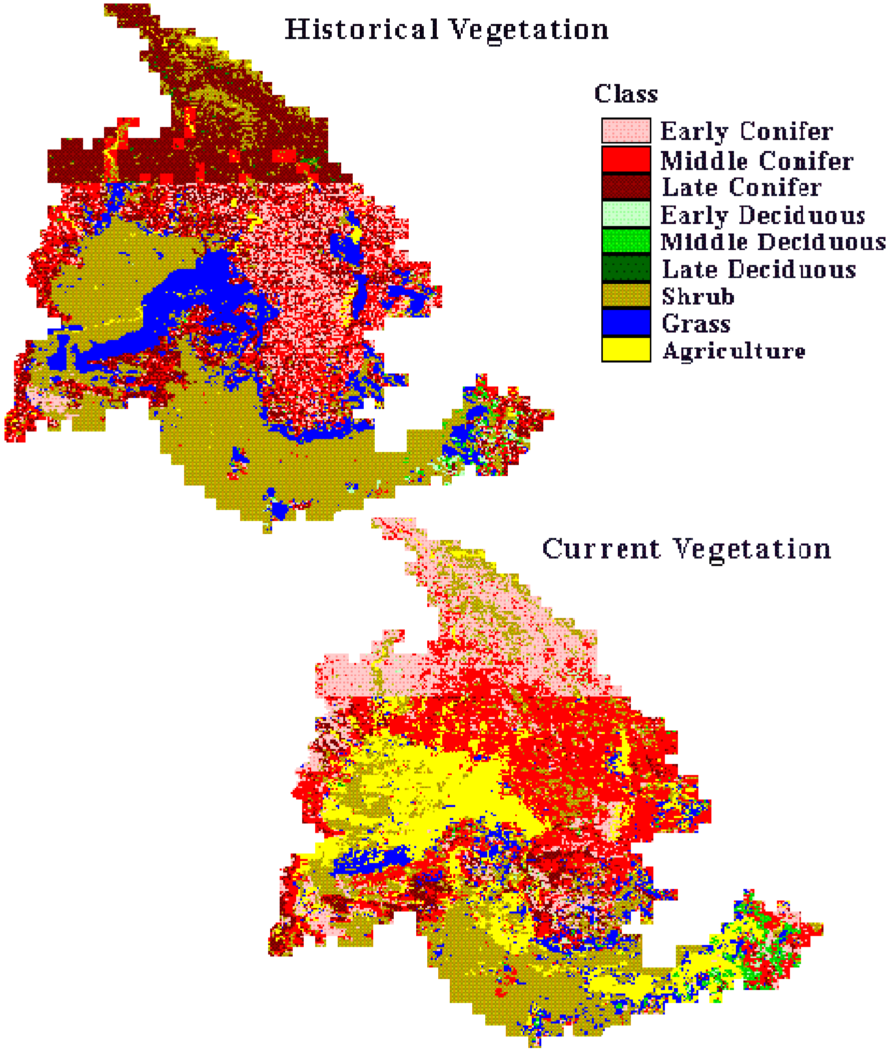

Fig. 7. Estimated Columbia River basin land cover for 1900 and 1990 (from Matheussen *et al.*, 2000).

snow interception capacity as a function of LAI. Changes in LAI are also reflected in the model's evapotranspiration algorithm (see Liang *et al.*, 1994 for details). Evaporative resistance of the vegetation and aerodynamic resistance are dependent on vegetation characteristics related directly or indirectly to LAI.

As shown in Fig. 7, summer LAI has generally been reduced along the northern periphery of the basin. Elsewhere, with the exception of parts of interior Idaho, there has generally been an increase in LAI. Within the forested areas of

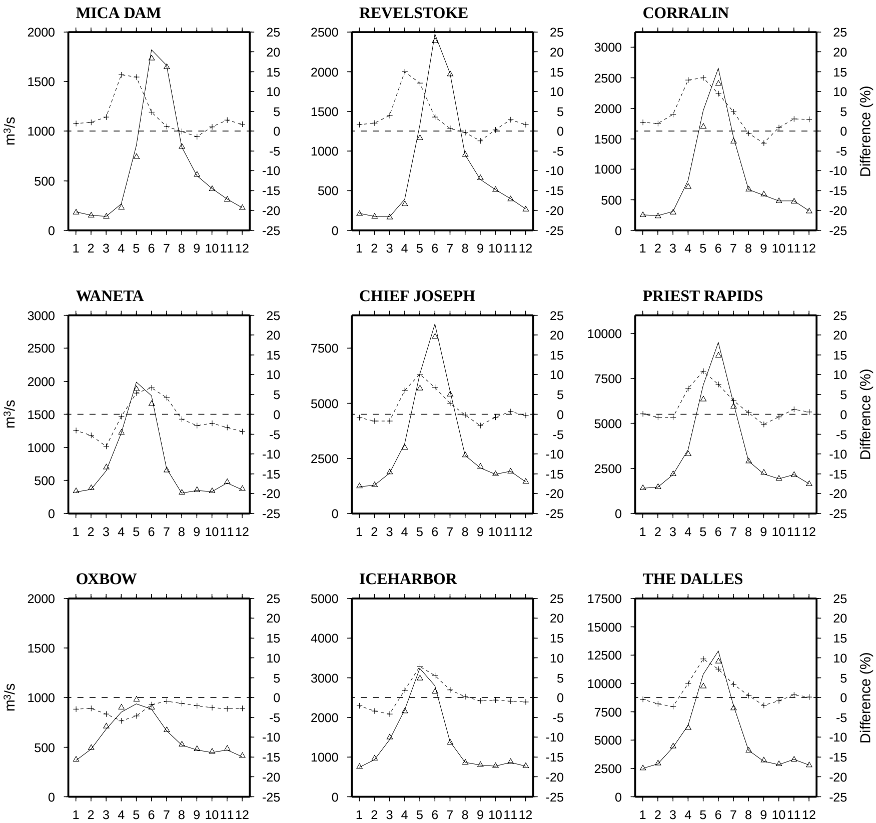

Fig. 8. Mean monthly hydrographs for current naturalized streamflow for nine locations in the Columbia River basin, and relative percentage change from historic conditions (from Matheussen *et al.*, 2000).

the basin, the two dominant causes of changes in LAI have been logging (which decreases mean LAI as the forest is "reset" to earlier structural stages) and fire suppression (which results in LAI increases as forests become more mature due to less frequent wildfires). In the remainder of the basin, increases in LAI most closely parallel the conversion of grasslands and shrublands to agriculture. Relative to grasslands and shrublands, agricultural land exhibits a stronger seasonal cycle of LAI that peaks in the summer. While the model represents changes due to increased LAI and related vegetative attributes for agricultural areas in the hydrologic simulations, it should be noted that it does not represent water management effects, such as irrigation.

Runoff at nine tributary locations throughout the basin was simulated for historical vegetation conditions. The predicted changes in runoff (expressed as relative percent difference) associated with the transition to current vegetation

Table 1. Mean changes in runoff by subbasin and season (in mm) associated with change from 1900 to 1990 vegetation in Columbia River basin (from Matheussen *et al*., 2000).

Runoff	JFM	AMJ	JAS	OND	Annual	Annual change (%)
Mica	2.1	36.2	2.4	3.2	43.9	4.2
Revelstone	1.3	37.3	–9.8	0.7	29.4	2.4
Corralin	1.6	38.5	1.8	1.9	43.9	7.1
Waneta	–4.1	11.4	–0.5	–1.6	5.2	1.4
Chief Joseph	–0.5	14.2	0.0	–0.3	13.4	3.0
Priest Rapids	2.1	18.1	2.4	1.9	24.4	10.7
Oxbow	–0.9	–1.7	–0.4	–0.6	–3.5	–2.9
Ice Harbor	–1.7	16.7	1.0	0.4	16.3	5.8
The Dalles	–0.8	2.6	–0.3	0.2	1.9	1.2

are shown in Fig. 8. For comparison, Table 1 summarizes the predicted incremental changes in evapotranspiration and runoff for each of the primary sub-basin locations. In the Columbia Basin, winter snow accumulation is the dominant source of runoff, and hydrographs from all of the primary tributary sites are strongly dominated by spring snowmelt. Consequently, changes in snow accumulation that might result from vegetation changes are expected to be a primary cause of the streamflow changes shown in Fig. 8. Figure 8 shows that flows during the spring snowmelt season increased at all locations by around 10 to 15%. On an annual average basis, the changes were somewhat less, typically in the range of 1–7%. Table 1 shows that the largest percentage changes were in the Corralin, Mica, Priest Rapids, and Ice Harbor reaches, which generally have the greatest predicted changes in snow accumulation. The exception to the dominant prediction of increasing streamflow is the Oxbow tributary in the upper Snake basin, where vegetation maturity was predicted to have increased, primarily due to the effects of fire suppression.

Changes in evapotranspiration are a secondary, although potentially important, mechanism affecting runoff. Matheussen *et al*. (2000) show that the predicted areas of highest maximum snow accumulation correspond to the areas of highest runoff generation. Comparison of changes in runoff production with maximum snow water equivalent changes suggests that most of the increases in snow accumulation are reflected in runoff, rather than in changes in evapotranspiration. This probably is because spring runoff occurs at a time when soil moisture is relatively high, therefore any additional snowmelt tends to contribute to runoff, rather than infiltration.

CASE STUDY 3: ENSEMBLE CLIMATE FORECASTING

In ensemble climate forecasting, a global land-atmosphere-ocean model (initialized with atmospheric, land surface and ocean conditions at forecast time), is run into the future for forecast horizons of months to years, using prescribed sea surface temperatures (SSTs) derived using one of a variety of forecast methods.

Although the atmosphere is essentially chaotic, the prescribed SSTs effectively constrain the evolution of model forecasts. By perturbing the initial conditions and repeating the simulation a number of times, an ensemble of forecasts is constructed which represents the range of global atmospheric conditions that may occur over the forecast period.

We describe an application in which the VIC hydrologic model is forced with climate ensemble forecast outputs to produce ensemble streamflow simulations from which a probability distribution of forecasted streamflow can be extracted. Ensemble climate forecasts (of precipitation and temperature) for six-month lead times produced by the NCEP/CPC Global Spectral Model (GSM) are used to force the VIC model at 1/8 degree spatial resolution over the eastern U.S. The coarse-scale GSM outputs (2.8125 degrees latitude by longitude grid mesh) were corrected for GSM regional bias, downscaled to 1/8 degree horizontal resolution and disaggregated to a daily time step for input to the VIC hydrologic model.

A comparison of the historically observed mean areal precipitation and temperature averaged over an Ohio River subbasin with the climate model values for the same area revealed a large summer precipitation model bias reaching 200% and temperature bias of 6 degrees Celsius (reversed in winter). In our experience with the Columbia River, biases of this magnitude are typical of climate model simulations (Leung *et al.*, 1999), and must be removed in order to produce realistic hydrologic simulations.

The bias correction step involves matching the quantiles of the GSM ensemble forecasts, relative to the GSM model climatology, to those of the observed climatology, to make the range of forecast model anomalies consistent with those of historically observed anomalies. Bias-corrected climate forecast anomalies are then interpolated to the finer hydrologic model scale. The subsequent imposition of a daily signal on the monthly anomaly forecasts is accomplished by resampling of the historic record, using a wet-dry classification of historic periods, and rescaling (for precipitation) or shifting (for temperatures) of the historic samples to reproduce the appropriate forecast anomaly. Wood *et al.* (2001) evaluate the bias correction and resampling approaches over the eastern U.S., and show that the procedure is able to reproduce reasonably well low order statistics (mean and variance) of the climatology.

Hydrologic model forecasts are produced by initializing VIC hydrology model states with a one-year spin-up period based on gridded observations (see Maurer *et al.*, 2001 for details). Following initialization, the bias corrected, downscaled ensemble forecasts (20 GSM forecast ensemble members produced by NCEP/CMB at the beginning of each month) are used to force the hydrology model through the end of the forecast period.

The forecast system was implemented over the eastern U.S. (defined as all of the U.S. east of the Mississippi River and Great Lakes drainage plus the Ohio River basin) for start dates from April through September, 2000 (Wood *et al.*, 2001). On or about the tenth of each month, a new set of ensemble forecasts was received from NCEP for a six-month forecast horizon. The gridded observed spin-up forcings for the VIC model were updated to the time of forecast, and the hydrologic ensemble forecasts were then generated. The period chosen for the study coincided with the early and middle part of a widespread drought in the southeastern United States.

Wood *et al.* (2001) evaluated the experimental forecast results using two types of forecast output: a) spatial plots of downscaled climate model forcings, and hydrological model predicted variables including runoff and soil moisture; and b) plots of predicted streamflow at selected USGS gaging stations where observations were available for model calibration. Spatial model output and streamflow were generated for each month of the six-month forecast horizon, for the six monthly forecast dates beginning in April, 2000.

The course of the southeastern drought is depicted in Fig. 9, which shows the retrospectively gridded precipitation and temperature and hindcast simulations of soil moisture and runoff that can be used as surrogate observations. Extremely low May precipitation coupled with high temperatures deepened drought conditions throughout the Ohio River Valley and the southeastern U.S., while the Northeast experienced slightly higher than average (with respect to the 1979–1999 climatology) precipitation. By July, temperatures along the east coast in the northern Ohio River Valley were cooler, and precipitation had risen to above normal in many locations, while the relative dryness and heat persisted from the Gulf Coast to the southern Ohio River Valley. September brought high temperatures everywhere except Florida and Georgia, and the region of low precipitation shifted north, while the precipitation deficit was less along the Gulf coast. In response to these forcings, predicted low soil moisture and runoff, which had been general over the entire domain south of New England, recovered gradually along the east coast and the northern Ohio River Valley, so that the center of the drought-stricken region, which initially included Florida, shifted to the west, over Alabama and Arkansas.

Figure 10 shows that the medians of the April ensemble climate forecasts were mostly above the median climatological precipitation in the southeast in May (month 1), and on the east coast (excepting Florida) in July (month 3), then below climatology everywhere except Florida in September (month 5). Above normal temperatures were forecast everywhere except Florida in May, in the mid-Atlantic states in July and in the southeast in September. Consequently, dry soil moisture and runoff would recover, according to the model predictions, in Florida and the mid-Atlantic states by July. In southern New England and the Ohio River valley, however, the forecast called for a continuation of dryness and heat, leading to low soil moisture and runoff in these regions. Figure 11 shows related streamflow ensemble forecasts (initialized in April, June, and August) for a stream location affected by the anomalies (Apalachicola River at Sumatra, FL) for the May–October, 2000 period.

In general, the broad features of the hydrology model forecasts for soil moisture and runoff were consistent with the precipitation and temperature signals produced by the climate forecasts. The climate forecast signals were modulated throughout summer by a rather large antecedent soil moisture deficit that resulted from abnormally low precipitation across much of the region, but

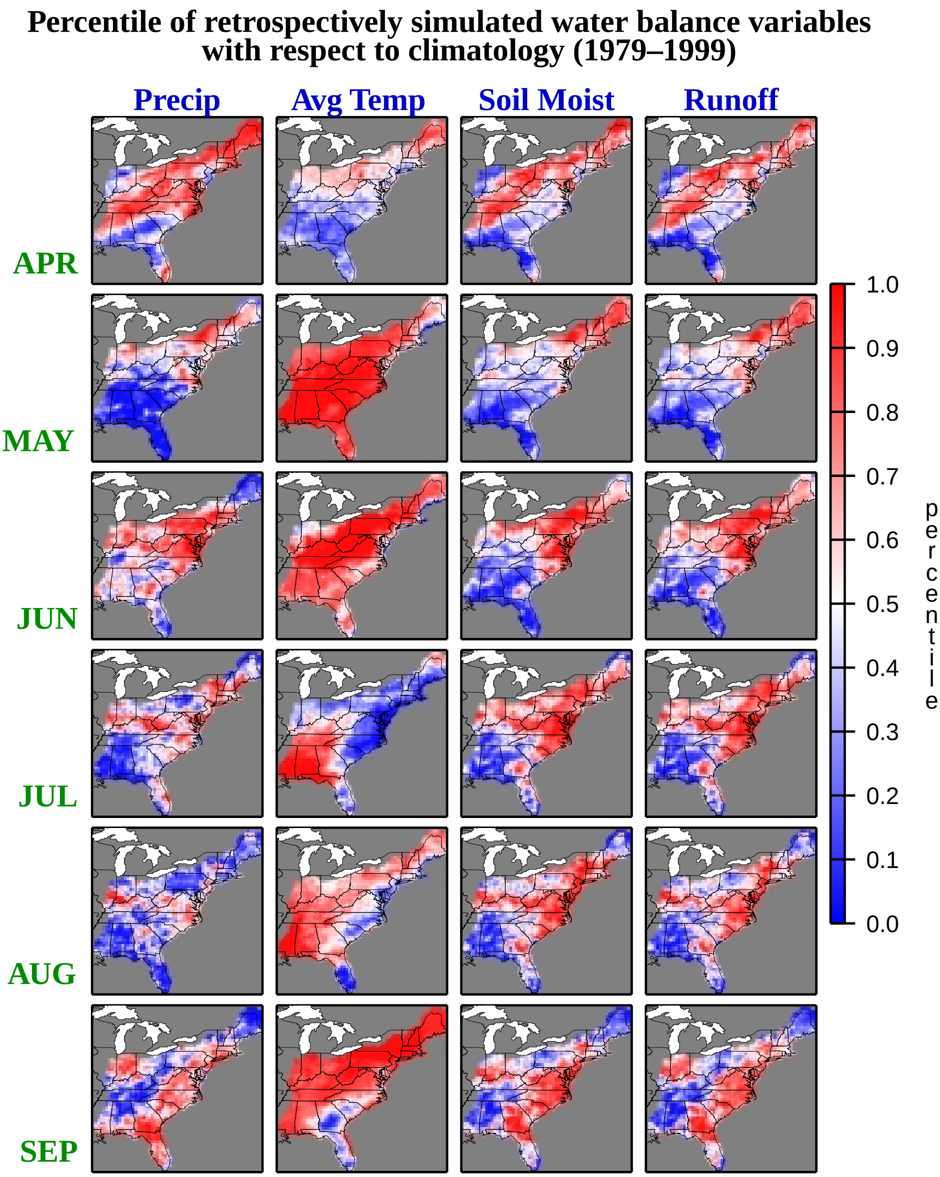

Fig. 9. April–September, 2000, gridded monthly total precipitation and monthly average temperature (derived from LDAS 1/8 degree land surface output), and monthly average soil moisture and monthly total runoff from VIC hindcast simulations, shown as percentiles of observed and simulated values, respectively, from the 21-year climatology period (from Wood *et al.*, 2001).

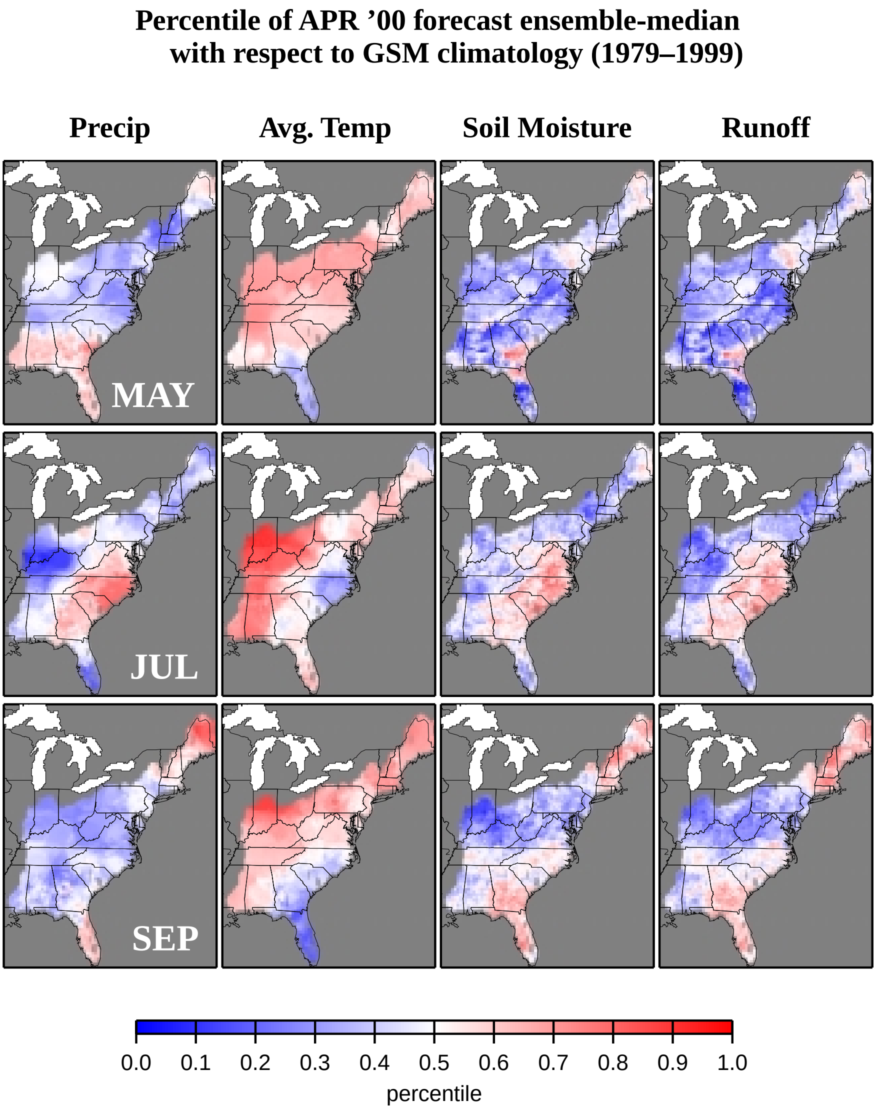

Fig. 10. April 2000 forecast ensemble medians for total precipitation, average temperature from GSM forecasts, and average soil moisture and total runoff from VIC simulations, for forecast months 1, 3, and 5, shown as a percentile of the 21-year climatology for each respective model (from Wood *et al.*, 2001).

particularly in the southeast, in winter and early spring, 2000. Simulated soil moisture resembled runoff anomalies were quite similar. Large variability in the forecast and climatology ensembles, however, may limit the significance of the results.

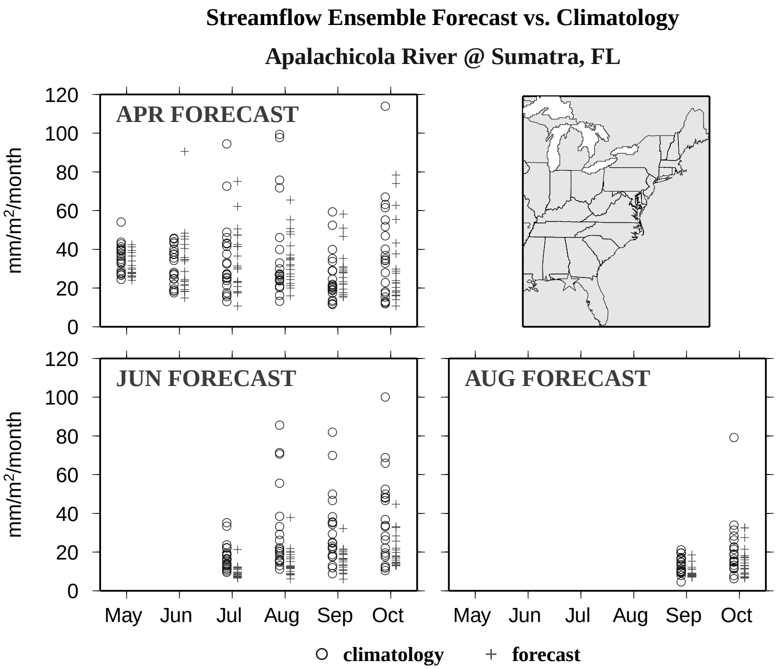

Fig. 11. April, June, and August 2000 forecast ensembles of monthly average streamflow (pluses) compared with simulated climatological values (circles), for the Apalachicola River at Sumatra, FL, for forecast months remaining in the study period. All four June forecasts, but only the first month of the August and April forecasts, were significantly different than climatology (from Wood *et al*., 2001).

CONCLUSIONS

Macroscale hydrologic models, applicable to large rivers and even continental scales, have advanced greatly in the last decade. As contrasted with more conventional hydrologic models applicable at the catchment scale where hydrologists have more traditionally focused, macroscale models are distinguished by a) explicit representation of vegetation, b) closure of both the surface energy and water budgets, and c) ability to reproduce observed surface hydrologic fluxes, especially streamflow. The first two features are common with most SVATS, and in fact there has been a convergence in the representation of (primarily) vertical energy transfer processes in macroscale hydrology models with those in SVATS. However, in contrast with SVATS, macroscale hydrology models focus more on the horizontal variations in surface properties, especially soils and topography, which influence the production of runoff. Three examples, detailing the use of the VIC macroscale hydrology model, have shown how such a macroscale model can be used to interpret the possible hydrologic effects of climate change on large rivers, to assess the hydrologic effects of vegetation change, and to exploit information in ensemble climate forecasts to produce probabilistic long-lead streamflow forecasts.

There remain, nonetheless, important challenges. The motivation for parameterization of subgrid processes is that the large scale effects of subgrid variability can be captured adequately if the probability distribution of the variability is specified. This implies that it is not necessary to represent specifically where within a grid cell a specific feature of either model forcings (e.g., precipitation) or surface characteristics (e.g., soil properties) occurs, but only its spatial probability distribution. Liang *et al*. (1996b) examined this assumption and found it justified in the case of representation of subgrid variations in precipitation. However, more work needs to be done to examine the limits of applicability of this assumption, especially with respect to the effects of scale.

Another challenge is to better determine how model parameters can best be determined directly from observations of surface characteristics. For instance, in the VIC model, soil moisture capacity is parameterized using a two-parameter probability distribution, where one parameter represents the spatially averaged soil moisture storage capacity, and the other is related to its spatial variability. Some success has been experienced in estimation of the spatial average moisture storage from soil maps or their equivalent, but the spatial variability parameter is harder to estimate, and in practice has usually been estimated using a calibration procedure. To the extent that model parameters can be estimated without the need to resort to calibration, greater confidence in the physical realism of the model, and its transferability, will result.

Finally, a key shortcoming in the structure of current macroscale hydrology models (and, for that matter, SVATS) is their failure to represent the effects of groundwater on land-atmosphere interactions. Beyond the practical implications (groundwater is the source of a substantial part of domestic water supplies globally), variations in groundwater storage can dominate those of the more active near surface soil moisture storage, and complicate accurate estimation of surface water budgets. Essentially all of the current generation of land surface schemes (both SVATS and macroscale hydrologic models) represents a near-surface soil column of depth less than one to a few meters, with no representation whatever of deeper groundwater, or the effects of recharge processes. More work is needed to implement groundwater representations consistent with the level of complexity in macroscale hydrology models, and/or to determine conditions under which groundwater processes can justifiably by ignored.

REFERENCES

Abdulla, F. A., Lettenmaier, D. P., Wood, E. F. and Smith, J. A. 1996. Application of a macroscale hydrologic model to estimate the water balance of the Arkansas-Red River basin, *J. Geophys. Res.*, **101**(D3), 7449–7459.

Arnell, N. W. 1999. The effect of climate change on hydrological regimes in Europe: a continental perspective, *Glob. Environ. Change,* **9**, 5–23.

Batjes, N. H. 1995. A homogenized soil data file for global environmental research: A subset of FAO, ISRIC, and NRCS profiles, Tech. Rep., International Soil Reference and Information Centre (ISRIC), Wageningen, The Netherlands.

Betts, A. K., Viterbo, P., Beljaars, A., Pan, H. L., Hong, S. Y., Goulden, M. and Wofsy, S. 1998. Evaluation of land-surface interaction in ECMWF and NCEP/NCAR reanalysis models over grassland (FIFE) and boreal forest (BOREAS), *J. Geophys. Res.-Atmos.*, **103**(D18), 23,079–23,085.

Bosch, J. M. and Hewlett, J. D. 1982. A review of catchment experiments to determine the effect of vegetation changes on water yield and evapotranspiration, *Journal of Hydrology*, **55**, 3–23.

Bowling, L. C. and Lettenmaier, D. P. 1997. Evaluation of the effects of forest roads on streamflow in Hard and Ware Creeks, Washington. Univ. Washington, Water Resources Series, Tech. Rep. No. 155, September.

Bras, R. A. 1990. *Hydrology, An Introduction to Hydrologic Science*, Addison Wesley, Inc., Reading, North Carolina.

Campbell, G. S. 1974. A simple method for determining unsaturated conductivity from moisture retention data, *Soil Sci.*, **117**, 311–314.

Chen, T. and 37 others 1997. Cabauw experimental results from the Project for Intercomparison of Land Surface Parameterisation Schemes (PILPS), *J. Climate*, **10**, 1194–1215.

Cherkauer, K. and Lettenmaier, D. P. 1999. Hydrological effects of frozen soils in the upper Mississippi River basin, *J. Geophys. Res.*, **106**(D16), 19,599–19,610.

Cosby, B. J., Hornberger, G. M., Clapp, R. B. and Ginn, T. R. 1984. A statistical exploration of the relationships of soil moisture characteristics to the physical properties of soils, *Water Resour. Res.*, **20**, 682–690.

Crawford, N. H. and Linsley, R. K. 1960. Computation of a synthetic streamflow record on a digital computer, *Int Assoc. Sci. Hydrol. Publication*, **51**, 526–538.

Dumenil, L. and Todini, E. 1992. A rainfall-runoff scheme for use in the Hamburg climate model, in *Advances in Theoretical Hydrology, A Tribute to James Dooge*, O'Kane, P., ed., European Geophysical Society Series on Hydrological Sciences 1, pp. 129–157.

FAO 1995. The digital soil map of the world, Version 3.5, CO-ROM avaiable from Food and Agriculture Organization of the United Nations; Viate delle terme di Caracalla, 00100 Rome, Italy.

Felzer, B. and Heard, P. 1999. Precipitation difference amongst GCMs used for the U.S. National Assessment, *J. Amer. Water Resour. Assoc.*, **35**, 1327–1340.

Gleick, P. H. 1999. Studies from the water sector of the National Assessment, *J. Amer. Water Resour. Assoc.*, **35**, 1297–1300.

Graham, S. T., Famiglietti, J. S. and Maidment, D. R. 1999. 5-minute, 1/2 degree, and 1 degree data sets of continental watersheds and river networks for use in regional and global hydrologic and climate system modeling studies, *Water Resour. Res.*, **35**, 583–587.

Hansen, M. C., DeFries, R. S., Townshend, J. R. and Sohlberg, R. 2000. Global land cover classification at 1 km spatial resolution using a classification tree approach, *Int. J. Remote Sens.*, **21**, 1331–1364.

Hardy, C. C., Burgan, R. E., Ottmar, R. D. and Deeming, J. E. 1996. A database for spatial assessments of fire characteristics, fuel profiles, and PM10 emissions, in *Compilation of Administrative Reports: Multi-Scale Landscape Dynamics in the Basin and Portions of the Klamath and Great Basins*, Keane, R. E., Jones, J. J., Riley, L. S. and Haan, W. J., tech. eds., on file with: *USDA, Forest Service, USDI, Bureau of Land Management; Interior Columbia Basin Ecosystem Management Project*, **112**, E. Poplar, Walla Walla, WA 99362.

Harr, R. D. 1986. Effects of clearcut logging on rain-on-snow runoff in western Oregon: New look at old studies, *Water Resour. Res.*, **22**(7), 1095–1100.

Hibbert, A. R. 1967. Forest treatment effects on water yield, in *Int. Symposium for Hydrology*, Sopper, W. E. and Lull, H. W., eds., Pennsylvania, Pergamon, Oxford.

Jarvis, P. G. 1976. The interpretation of the variations in leaf water potential and stomatal conductance found in canopies in the field, *Philosophical Transactions of the Royal Society*, **273**, 593–610.

Johansen, O. 1975. Thermal conductivity of soils, Ph.D. Thesis, Trondheim, Norway.

Jones, J. A. and Grant, G. E. 1996. Peak flow responses to clear-cutting and roads in small and large basins, western Cascades, Oregon, *Water Resour. Res.*, **32**, 959–974.

Kalnay, E., Kanamitso, M., Kistler, R., Collins, W., Deaven, D., Gandin, L., Iredell, M., Saha, S., White, G., Woolen, J., Zhu, Y., Leetma, A., Reynolds, R., Chelliah, M., Ebisuzaki, W., Higgins, W., Janoviak, J., Mo, K. C., Jenne, R. and Joseph, D. 1996. The NCEP/NCAR 40-year reanalysis project, *Bulletin of the American Meteorological Society*, **77**, 437–471.

Kimball, J. S., Running, S. W. and Nemani, R. 1997. An improved method for estimating surface humidity from daily minimum temperature, *Agric. For. Meteor.*, **85**, 87–98.

Kirschbaum, R. L. and Lettenmaier, D. P. 1997. An evaluation of the effects of anthropogenic activity on streamflow in the Columbia River Basin, University of Washington, Department of Civil Engineering Water Resources Series Technical Report No. 156.

Koster, R. D. and Milly, C. D. 1997. The interplay between transpiration and runoff formulations in land surface schemes used with atmospheric models, *J. Climate*, **10**(7), 1578–1591.

Leung, L. R., Hamlet, A. F., Lettenmaier, D. P. and Kumar, A. 1999. Simulations of the ENSO hydroclimate signals in the Pacific northwest Columbia River basin, *Bulletin of the American Meteorological Society*, **80**(11), 2313–2329.

Liang, X., Lettenmaier, D. P., Wood, E. F. and Burges, S. J. 1994. A simple hydrologically based model of land surface, water, and energy fluxes for general circulation models, *J. Geophys. Res.*, **99**(D7), 14,415–14,428.

Liang, X., Lettenmaier, D. P. and Wood, E. F. 1996a. One-dimensional statistical dynamic representation of subgrid spatial variability of precipitation in the two-layer variable infiltration capacity model, *J. Geophys. Res.*, **101**(D16), 21,403–21,422.

Liang, X., Wood, E. F. and Lettenmaier, D. P. 1996b. Surface soil moisture parameterization of the VIC-2L model: Evaluation and modifications, *Global and Planetary Change*, **13**, 195–206.

Liang, X., Wood, E. F. and Lettenmaier, D. P. 1999. Modeling ground heat flux in land surface parameterization schemes, *J. Geophys. Res.*, **104**(D8), 9581–9600.

Lohmann, D., Raschke, E., Nijssen, B. and Lettenmaier, D. P. 1998a. Regional scale hydrology: I. Formulation of the VIC-2L model coupled to a routing model, *Hydrological Sciences - Journal - des Sciences hydrologiques*, **43**(1), 131–141.

Lohmann, D., Raschke, E., Nijssen, B. and Lettenmaier, D. P. 1998b. Regional scale hydrology: II. Application of the VIC-2L model to the Weser River, Germany, *Hydrological Sciences - Journal - des Sciences hydrologiques*, **43**(1), 143–158.

Matheussen, B., Kirschbaum, R. L., Goodman, I. A., O'Donnell, G. M. and Lettenmaier, D. P. 2000. Effects of land cover change on streamflow in the interior Columbia Basin, *Hydrological Processes*, **14**(5), 867–885.

Maurer, E. P., O'Donnell, G. M., Lettenmaier, D. P. and Roads, J. O. 2001a. Evaluation of NCEP/NCAR reanalysis water and energy budgets using macroscale hydrologic model simulations, in *Land Surface Hydrology, Meteorology, and Climate: Observations and Modeling*, Lakshmi, V., Albertson, J. and Schaake, J., eds., American Geophysical Union, pp. 137–158.

Maurer, E. P., O'Donnell, G. M., Lettenmaier, D. P. and Roads, J. O. 2001b. Evaluation of the land surface water budget in NCEP/NCAR and NCEP/DOE AMIP-II reanalyses using an off-line hydrologic model, *Journal of Geophysical Research*, Nov. (to appear).

McCumber, M. C. and Pielke, R. A. 1981. Simulation of the effects of surface fluxes of heat and moisture in a mesoscale numerical model, *J. Geophys. Res.*, **86**(C10), 9929–9938.

Nijssen, B., Lettenmaier, D. P., Liang, X., Wetzel, S. W. and Wood, E. F. 1997. Streamflow simulation for continental-scale river basins. *Water Resour. Res.*, **33**(4), 711–724.

Nijssen, B., Lettenmaier, D. P., Lohmann, D. and Wood, E. F. 2001a. Predicting the discharge of global rivers, *J. Climate* (in press).

Nijssen, B., Schnur, R. and Lettenmaier, D. P. 2001b. Global retrospective estimation of soil moisture using the variable infiltration capacity land surface model, 1980–93, *Journal of Climate*, **14**(8), 1790–1808.

Nijssen, B., O'Donnell, G. M., Hamlet, A. F. and Lettenmaier, D. P. 2001c. Hydrologic sensitivity of global rivers to climate change, *Climatic Change* (in press).

O'Donnell, G. M., Czajkowski, K. P., Dubayah, R. O. and Lettenmaier, D. P. 2000. Macroscale hydrological modeling using remotely sensed inputs: Application to the Ohio River Basin, *J. Geophys. Res.*, **105**(D10), 12,499–12,516.

Peters-Lidard, C. D., Blackburn, E., Liang, X. and Wood, E. F. 1998. The effect of soil thermal conductivity parameterization on surface energy fluxes and temperatures, *Journal of the Atmospheric Sciences*, **55**(7), 1209–1224, 1998.

Pitman, J. and 25 others 1993. Results from the off-line control simulation phase of the Project for Intercomparison of Land Surface Parameterisation Schemes (PILPS), GEWEX technical note, IGPO Publication Series, 7, 47 pp.

Quigley, T. M. and Arbelide, S. J. (tech. eds.) 1997. An assessment of the ecosystem components in the interior Columbia Basin and portions of the Klamath and Great Basins: Vol. 2. General. Technical Report, PNW-GTR-405. Portland, OR.

Row, L. W., Hastings, D. A. and Dunbar, P. K. 1995. TerrainBase worldwide digital terrain data documentation manual, National Geophysical Data Center, Boulder, CO.

Shuttleworth, W. J. 1996. GCIP Coupled Modeling Workshop, IGPO publication Series No. 23, Silver Spring, MD, 20 pp.

Stednick, J. D. 1996. Monitoring the effects of timber harvest on annual water yield, *Journal of Hydrology*, **176**, 79–95.

Storck, P. 2000. Trees, snow and flooding: An investigation of forest canopy effects on snow accumulation and melt at the plot and watershed scales in the Pacific Northwest, Water Resources Series Technical Report No. 161, Department of Civil and Environmental Engineering, University of Washington.

Storck, P. and Lettenmaier, D. P. 1999. Predicting the effect of a forest canopy on ground snow accumulation and ablation in maritime climates, in *Proc. 67th Western Snow Conf.*, Troendle, C., ed., pp. 1–12, Colorado State University, Fort Collins.

Thornton, P. E. and Running, S. W. 1999. An improved algorithm for estimating incident daily solar radiation from measurements of temperature, humidity, and precipitation, *Agric. For. Meteor.*, **93**, 211–228.

Todini, E. 1996. The ARNO rainfall-runoff model, *Journal of Hydrology*, **175**, 339–382.

Wigmosta, M. S., Vail, L. W. and Lettenmaier, D. P. 1994. A distributed hydrology-vegetation model for complex terrain, *Water Resour. Res.*, **30**(6), 1665–1669.

Wood, A. W., Maurer, E. and Lettenmaier, D. P. 2001. Evaluation of the hydrologic use of ensemble climate forecasts, application to Eastern U.S. for summer, 2000, *J. Geophys. Res.* (in review).

Wood, E. F. 1991. Global scale hydrology: Advances in land surface modeling, *Reviews of Geophysics Supplement*, 193–201.

Wood, E. F., Lettenmaier, D. P., Liang, X., Nijssen, B. and Wetzel, S. W. 1997. Hydrological modeling of continental-scale basins, *Annual Review of Earth and Planetary Sciences*, **25**, 279–300.

Wood, E. F., Lettenmaier, D. P., Liang, X., Lohmann, D., Boone, A., Chang, S., Chen, F., Dai, Y., Dickinson, R. E., Duan, Q., Ek, M., Gusev, Y. M., Habets, F., Irannejad, P., Koster, R., Mitchel, K. E., Nasonova, O. N., Noilhan, J., Schaake, J., Schlosser, A., Shao, Y., Shmakin, A. B., Verseghy, D., Warrach, K., Wetzel, P., Xue, Y., Yang, Z. L. and Zeng, Q. 1998. The Project for Intercomparison of Land-Surface Parameterization Schemes (PILPS) Phase-2(c) Red-Arkansas River experiment: 1. Experiment description and summary intercomparisons, *Journal of Global and Planetary Change*, **19**, 115–135.

Zhao, R. J., Zhang, Y. L., Fang, L. R., Liu, X. R. and Zhang, Q. S. 1980. The Xinanjiang model, in *Hydrological Forecasting Proceedings Oxford Symposium*, IASH **129**, 351–356.

D. P. Lettenmaier (e-mail: dennisl@u.washington.edu)